

Morphology and growth mechanism of single-helix spring-like carbon nanocoils with laces prepared using Ni/molecular sieve (Fe) catalyst

X. CHEN*, K. TAKEUCHI, S. YANG, S. MOTOJIMA**

Department of Applied Chemistry, Faculty of Engineering, Gifu University, Gifu, 501-1193, Japan

*Email: xqchen39@hotmail.com,

**Email: motojima@apchem.gifu-u.ac.jp

Published online: 3 March 2006

Single-helix spring-like carbon coils with laces grew over the Ni metal catalyst supported on molecular sieve containing a trace amount of an Fe impurity that originated from a kaolin clay raw material. The morphology, microstructure, and growth mechanism of the single-helix carbon nanocoils and laces were investigated. We found that a trace amount of Fe impurity contained in the molecular sieve was a key factor in the lace growth. It is considered that the Fe impurity may poison, restraint the formation of three crystal faces, resulting in the growth of single helix coils. It is also considered that a very strong inner stress is periodically formed between the boundary of two fibers, and the thin carbon film is swelled to form laces.

© 2006 Springer Science + Business Media, Inc.

1. Introduction

As early as the 1930s, it was recognized that the presence of highly charged cations on an oxide surface altered the catalytic properties of supported metals for the vapor growth of carbon fibers [1]. Smaller catalyst particles can be achieved by dispersing the catalyst particles on a substrate (supporter), and the supporter can also influence the catalyst performance through an electronic interaction, i.e., strong metal support interaction (SMSI), which is a benefit for achieving an exposed catalyst plane in favor of the carbon fiber growth. Recently, there have been many reports about controlling the size and growth density of carbon nanotubes (CNTs) by dispersing the catalyst particles on supporters [2–4]. However, lower yields of the carbon deposits than that using a non-supported metal catalyst were generally obtained [4]. On the other hand, molecular sieve are a kind of new catalyst supporter with many interesting properties [5]. However, there are some disagreements on this aspect [6, 7].

Motojima *et al.* added a small controlled amount of sulfur impurities to the chemical vapor deposition (CVD) process of the acetylene pyrolysis over a Ni catalyst, and found that sulfur could dramatically promote the

growth of helically coiled carbon fibers (carbon microcoils, CMCs) with a coil diameter of several micrometers [8, 9]. This discovery enables carbon microcoils to be synthesized in high purity and on a large scale with a high reproducibility.

Some researchers have reported the synthesis of carbon nanocoils, for example, Nakayama group reported preparation of tubule nanocoils in high yield using iron-coated indium tin oxide as catalyst [10, 11]. Motojima group prepared carbon nanocoils using sputtered films of Au or Au/Ni as the catalyst [12]. Recently, we found that by using a supported catalyst and controlling the CVD conditions, the carbon nanocoils with various conformations could be obtained using a Ni catalyst supported on Al₂O₃ powder [13]. We also found that single-helix twisted nanocoils and single-helix spring-like carbon micro/nanocoils (occasionally with laces) could be prepared over Fe-Cr containing alloys (stainless steel series) [14, 15]. The carbon nanocoils are basically different from the helix-shaped carbon nanotubes reported in Refs. [2–4]. The former have almost an amorphous structure and do not have a central tube-like pore in the fiber axis, while the latter is crystalline with a central thin tube in the fiber

*Author to whom all correspondence should be addressed.

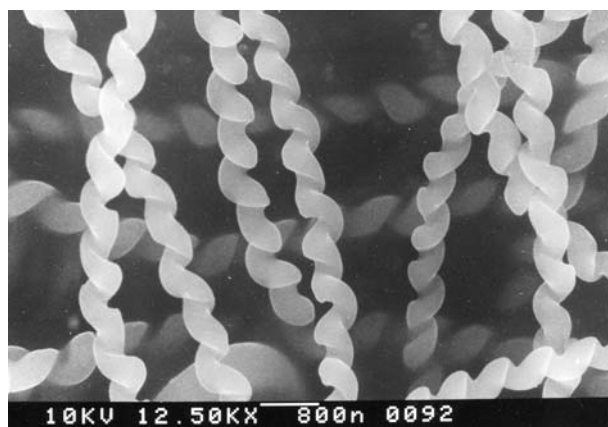


Figure 1 SEM image of single-helix twisting carbon nanocoils.

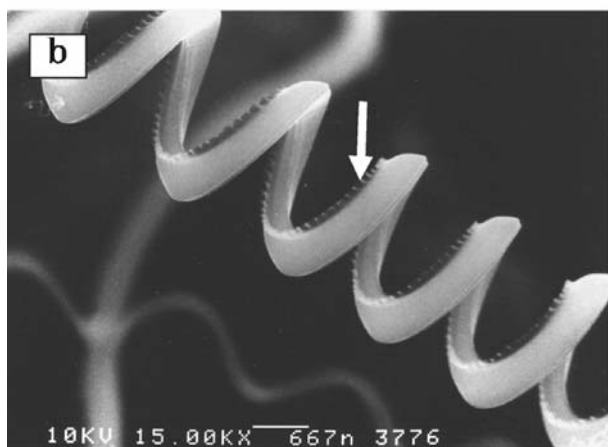
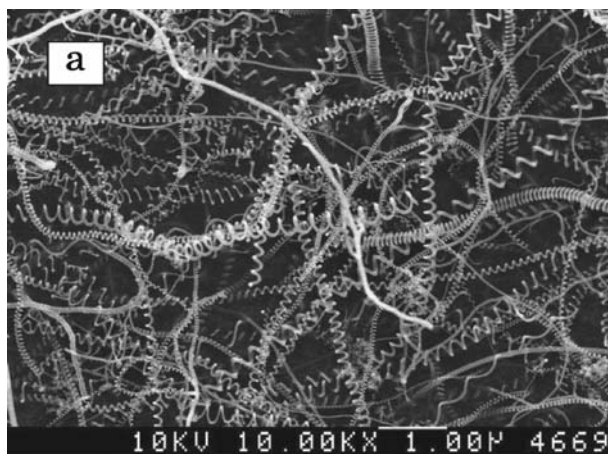


Figure 2 SEM images of single-helix carbon nanocoils (a) and the enlarged view (b). Arrow in Fig. 1(b) indicates laces.

axis. The carbon nanocoils have a 3D-helical structure with nanometer-ordered coil diameters and thus are expected to be used as novel electromagnetic wave absorbers in the GHz to THz regions, ultraviolet ray absorbers, micro-antennas, micro/nano-sensors or nano-actuators, activators of skin cell propagation or metabolism, etc.

In this study, single-helix carbon nanocoils with various laces patterns on the surface were prepared by the catalytic

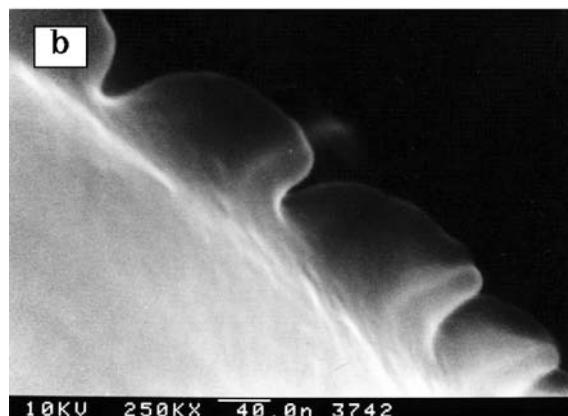
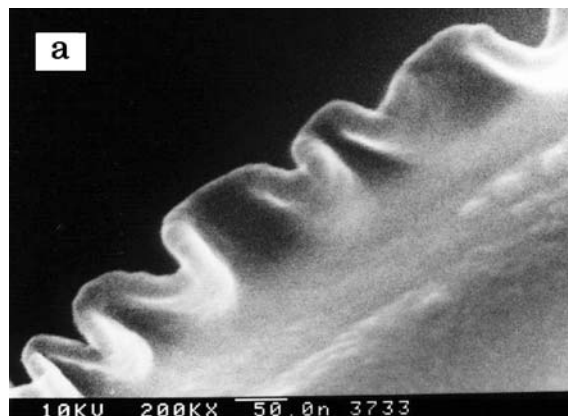


Figure 3 Enlarged view of the laces.

pyrolysis of acetylene using a Ni metal catalyst supported on molecular sieve containing a trace amount of Fe impurity that originated from a kaolin clay raw material. The morphology, microstructure, and growth mechanism of the single-helix carbon nanocoils and laces were investigated. To our knowledge, up till now, there has been no report about carbon nanocoils with laces by other research groups.

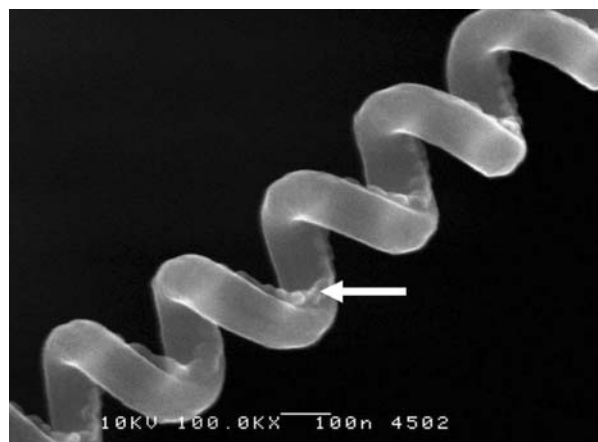


Figure 4 SEM image of a single-helix carbon nanocoil with laces (arrow).

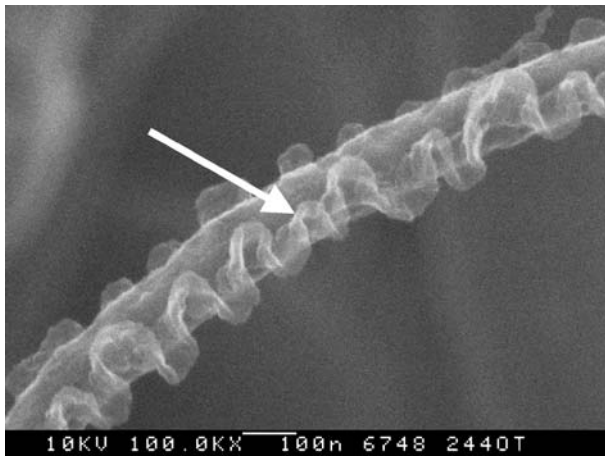


Figure 5 SEM image of a straight carbon fiber with laces (arrow).

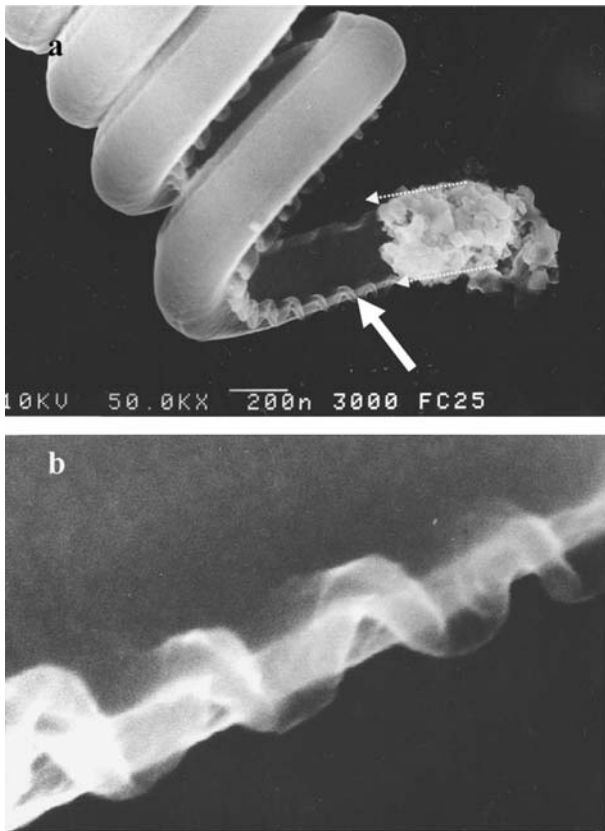


Figure 6 Growth tip of a single-helix carbon nanocoil with wave-like laces (a) and the enlarged view (b).

2. Experimental

Nickel supported on molecular sieve, which was prepared from kaolin clay materials containing a trace amount of Fe metal, was prepared by an impregnation method using $\text{Ni}(\text{NO}_3)_2 \cdot 6\text{H}_2\text{O}$ as a precursor as follows: aqueous solutions of a $\text{Ni}(\text{NO}_3)_2 \cdot 6\text{H}_2\text{O}$ were mixed with molecular sieve powder, which was prepared using Fe-containing kaolin as the raw material, stirred for 2 h at 60°C to remove the dissolved oxygen to achieve a homogeneous impregnation of the metal salts in the support. The impregnation

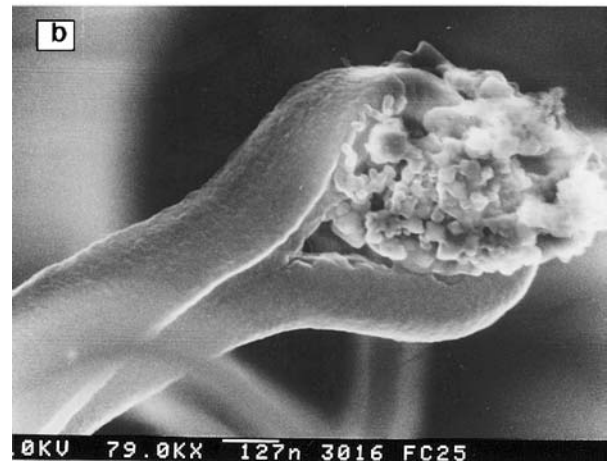
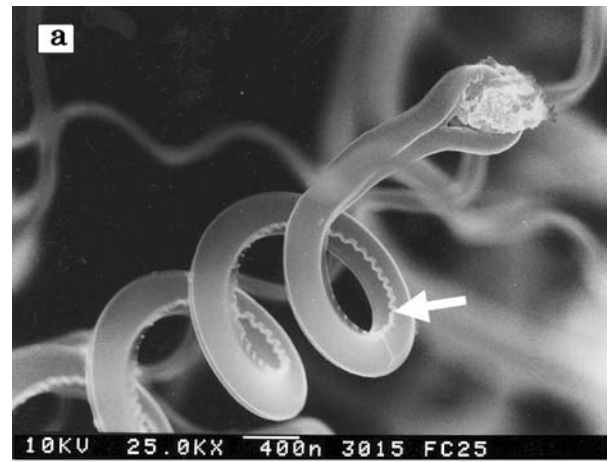


Figure 7 Hamburger-like growth tip of a single-helix carbon nanocoil with wave-like laces (a) and the enlarged view (b). Arrow indicates catalyst grains.

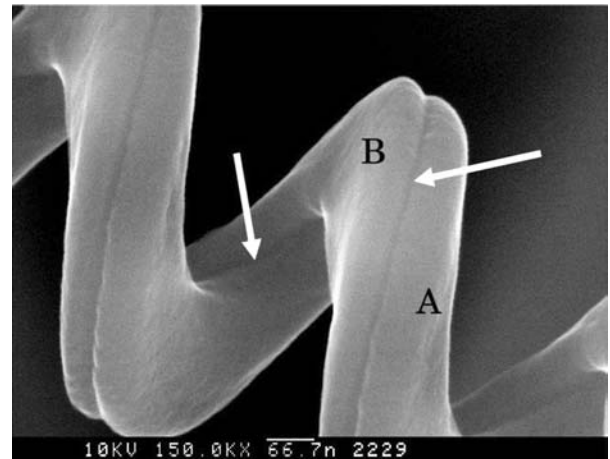


Figure 8 Single-helix carbon nanocoil without a lace. Arrows indicates dent lines. A and B indicate two parts of carbon fibers.

deposits were then dried in an oven at 100°C for 12 h, calcined at 500°C for 3 h. The atomic ratio of Fe against Ni in the catalyst deposits (referred to as molecular sieve (Fe) hereafter) was about 10%.

The carbon nanocoils were obtained by the catalytic pyrolysis of acetylene containing a trace amount of

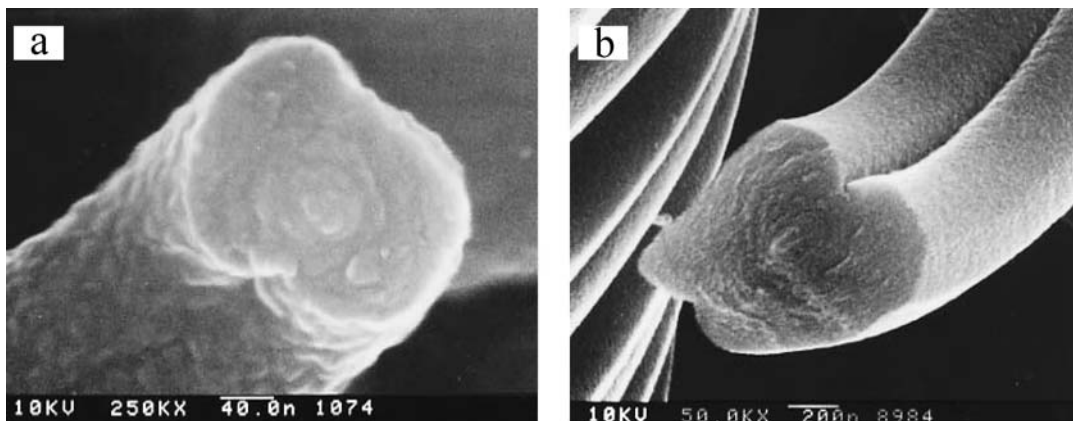


Figure 9 Ruptured cross section of the single-helix carbon nanocoils without lace.

hydrogen sulfide as an impurity, which acts as a promoter. A vertical quartz tube (6×10^{-2} m, i.d.), which has an upper source gas inlet and a lower gas outlet, was used as the reaction tube. The catalyst powders (Ni/molecular sieve (Fe)) of ca. 2 mg/cm^2 -substrate were uniformly dispersed on a graphite substrate plate, which was placed in the central region of the reaction tube. The reaction tube was heated by nichrome elements from the outside. The catalyst was first reduced and activated at 700°C for 1 h in a H_2 flow just before the reaction was started. A source gas mixture of acetylene, H_2 and N_2 (sometimes flow rate is zero) was then vertically introduced onto the substrate surface through the upper gas inlet and exhausted through the lower gas outlet; the pressure within the reaction tube was atmospheric. The reaction temperature and the gas flow rates of C_2H_2 , $\text{H}_2\text{S}/\text{H}_2$, H_2 , and N_2 , were $760\text{--}780^\circ\text{C}$, $30\text{--}150$ sccm, $10\text{--}200$ sccm, $50\text{--}550$ sccm, and $0\text{--}100$ sccm, respectively. The samples used for the observations or examinations were mainly collected from the central parts of the substrates. High-resolution FE-SEM (TOPCON, ABT-150F) and TEM (HITACHI, H-8100) were employed to examine their morphologies and microstructures, respectively.

3. Results and Discussion

There were mainly three kinds of morphologies of the carbon nanocoils produced by this catalyst; a) single-helix twisting carbon nanocoils; b) single-helix spring-like carbon coils with laces; and c) single-helix spring-like carbon nanocoils without laces. However, when the reaction conditions were controlled as follows: the reaction temperature and the gas flow rates of C_2H_2 , $\text{H}_2\text{S}/\text{H}_2$, H_2 , and N_2 , were 780°C , $30\text{--}60$ sccm, $20\text{--}50$ sccm, $100\text{--}150$ sccm, and $0\text{--}50$ sccm, respectively, the deposits were mainly spring-like single-helix carbon nanocoils.

The representative SEM images of the single-helix twisting carbon nanocoils are shown in Fig. 1. The carbon fibers of about 350 nm fiber diameter twists with a twisting (coil) diameter of about 600 nm formed twisted nanocoils. The representative SEM images of the single-helix carbon nanocoils are shown in Fig. 2. Among all

of the grown carboncoils, single-helix carbon nanocoils (in appearance) were the most frequently observed. The diameter of the fiber (from which a coil was built) ranged from 100 to 500 nm with the average being $150\text{--}300 \text{ nm}$. The coil diameter ranged from 200 to $3,000 \text{ nm}$, and the highest probability was $1,000\text{--}2,500 \text{ nm}$. The coil yield in the substrate area was $0.01\text{--}0.03 \text{ g/cm}^2$ -substrate, while the coil yield versus C_2H_2 feed was 2% , which is much lower than that described in [13].

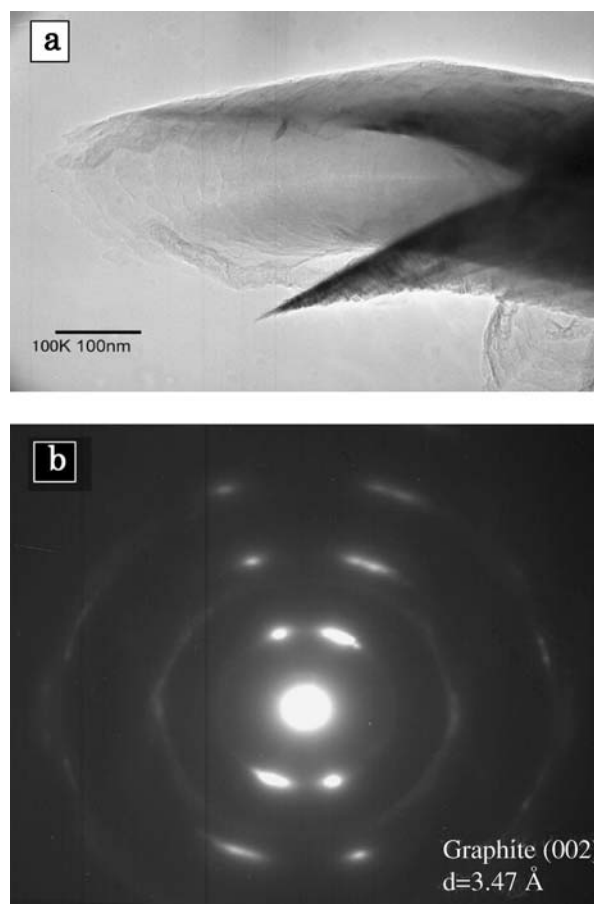


Figure 10 TEM image of the ruptured cross section of a single-helix carbon nanocoil after heat treatment at 2500°C for 8 hrs (a), and the electron diffraction pattern (b).

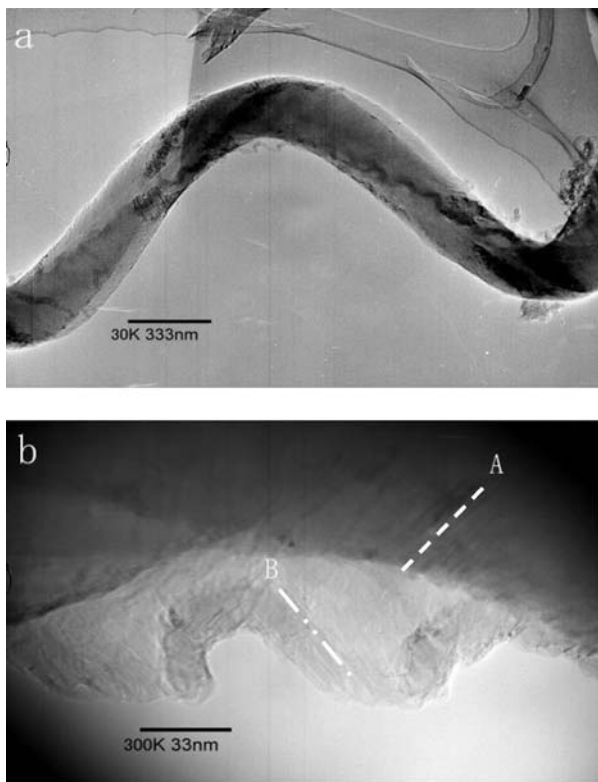


Figure 11 TEM image of a single-helix carbon nanocoil with a lace after heat treatment at 2500°C for 8 hrs (a), and the enlarged view of the lace (b). Lines A and B indicate that the graphite layer of the lace is in a different direction to that of the bulk fiber.

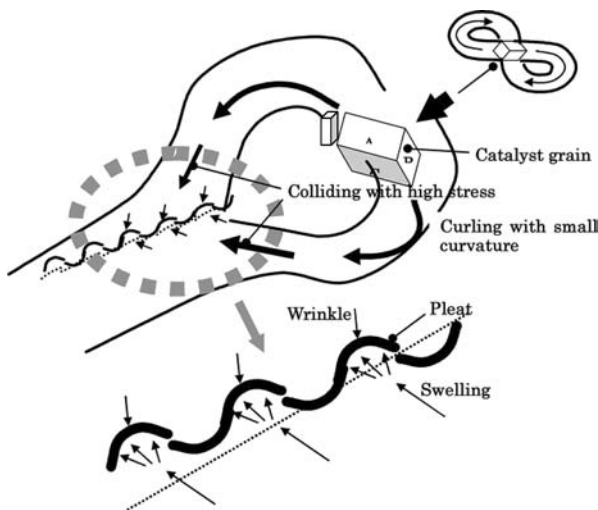


Figure 12 Growth mechanism of a single-helix carbon nanocoil and the laces.

However, it was very interesting to find that when the nitrogen flow rate was zero, the growth of lace-like continuous ribbons (referred to as a lace) was generally observed on the surface of the fiber. The enlarged views of a nanocoil with the laces are shown in Figs. 2–3. From an enlarged view, the fiber diameter, coil diameter, coil pitch, and lace height (or width) were about 500, 2, 500, 1,500, and 70–75 nm, respectively. The laces have various kinds of morphologies; i.e., wave-form or the Great-Wall

type (a), gear type (b), etc. Fig. 4 shows a nanocoil with a smaller coil diameter than that in Fig. 2b; the fiber diameter, coil diameter, coil pitch, the lace height (or width) were about 100, 300, 300, and 20 nm, respectively. It was found that the coil pitch size of the single-helix carbon nanocoils was generally nearly the same as the coil diameter size. This morphological characteristic is very special, and has not been observed in double-helix carbon microcoils [8].

We have reported that the electrical resistivity, inductance and capacitance of double-helix carbon microcoils (CMCs) changed by extending or contacting along the coil length [16], and thus the CMC composites in which 1–3 wt% CMC was uniformly embedded in the elastic polysilicone were used as tactile sensors. It is considered that the spring-like carbon nanocoils can change the mechanical and electrical properties more effectively under applied external energies such as mechanical and electrical fields than that of CMC. Accordingly, the single-helix coils are expected to have very novel and outstanding sensor properties and can be used in Micro Electro Mechanical Systems (MEMS), etc. The sensor properties will be presented in another paper. On the other hand, the characterization of the single-helix spring-like carbon coils with laces is being investigated. For example, they have higher surface areas than those without laces, thus they are expected to be used as gas absorption materials.

Some straight carbon nanofibers, that were grown mixed with the single helix carbon nanocoils, also had lacescoalesced on the surface. An example is shown in Fig. 5, in which the fiber diameter is about 150 nm and the lace height is about 25 nm.

Very interesting tip morphologies of the single-helix carbon nanocoils with laces were often observed. Some examples are shown in follows. Fig. 6a shows a growth tip of the single-helix carbon nanocoil with a right-clockwise coiling pattern and with laces having a zigzag pattern on the surface of the fiber, indicating that these kinds of coils grew by a mono-directional growth mode from a seed (catalyst) particle. The seed particle may consist of many fine catalyst particles, which may contain four elements of C, M (catalyst metal), O, and S, as in the case of the CMCs [17]. The two arrays of laces grew from two sides of the catalyst seeds as shown by the dotted arrows. Furthermore, the two lace arrays also continuously grew on the edge of the dent formed on the inner side of the coils as shown in Fig. 6a (thick arrow). Fig. 7 shows another type of growth tip. A catalyst grain (arrow) is enclosed by two parts of the fiber (i.e., 2 sub-fibers). That is, two fibers grown from the both sides of the catalyst grain and then coalesced to form one fiber coiling with a left-clockwise coiling pattern. There is only one lace on the edge of the inner dent of the nanocoil except for the tip part (unlike that of Fig. 6). The fiber diameter, coil gap, coil diameter are about 300, 400–500, and 1,500 nm respectively. On the other hand, it was observed that for the carbon nanocoils without laces, two striations with

various depths were observed on the surface along the fiber axis. A representative nanocoil without a lace is shown in Fig. 8, in which the fiber diameter and the coil diameter are about 170 nm and 700 nm respectively. The two striation lines (arrows), where no lace array was observed on the fiber surface, can be clearly seen. Are these single coils (in appearances) without lace pure single coils, which are composed from a single piece of carbon fiber, or are they composed of two coils adherently coalesced? Fig. 9 shows two ruptured cross sections of the single coils with shallow and deep striations on the fiber surfaces. If the single coil was composed of two coalesced coils, two negative or positive cones should be observed in the central part of the respective fibers from which the coils are formed. However, in fact, only one negative cone can be seen in the central part of the fibers irrespective of the striation thickness. Accordingly, these observations suggest that these single coils without lace are composed from a piece of carbon fiber. On the other hand, the single coils with a lace, such as shown in Fig. 6, are plausibly formed from two fibers adherently coalesced or fused together.

A TEM image and selected area electron diffraction pattern of a cross section of the single-helix carbon nanocoils are shown in Fig. 10. The growth of thin platelets, which is in a small angle (ca. 20–30 deg) to the fiber axis, was observed. They are similar to that of the heat-treated CMCs [18]. The electron diffraction pattern showed that the apparent graphite diffraction pattern of the (0002), indicated good development of the graphite layers with a layer distance of 0.347 nm (Fig. 10b). That is, the single-helix carbon nanocoils have a herring-bone structure, suggesting that the nanocoils have a more ordered microstructure than that of the double-helix carbon microcoils, which are almost amorphous. It was observed that the single-helix coiling pattern was completely retained even after the heat-treatment at 2500°C for 8 hrs in an N₂ atmosphere.

Fig. 11 shows a TEM image of a heat-treated single-helix carbon nanocoil with a wave-like lace, indicating that it has a lace coalescing to its bulk. From Fig. 11b, it can be seen that the direction (B) of the graphite layers developed in the lace part is different from that of the bulk fiber (A).

Using a Ni metal catalyst, two fibers usually grow from a catalyst grain in an opposite direction and entwine each other to form double-helix carbon coils [17]. The catalyst grain is a Ni₃C single crystal and has six crystal faces in the ideal case. That is, two fibers grow from six crystal faces of the Ni catalyst grain. On the other hand, using a Ni/molecular sieve (Fe) catalyst, there is usually only one fiber which grows from a catalyst grain to form a single-helix carbon nanocoil. That is, among the six crystal faces of the Ni catalyst grain, three faces do not contribute to the carbon coil formation. EPMA results indicated that the molecular sieve contained a trace amount of an Fe impurity that originated from the kaolin clay raw material. It may be postulated that the Fe impurity poisons the formation of three crystal faces of the Ni catalyst grain

and only a carbon fiber is formed from the remaining three crystal faces, resulting in a single-helix carbon nanocoil. However, it is observed that an actual catalyst grain is not a single crystal but is composed of polycrystals as shown in Figs. 6a or 7a, and thus the mechanism described above cannot be directly applied, but needs some modification. A possible growth mechanism of the single-helix nanocoils of Fig. 7 is proposed as shown in Fig. 12. The Fe impurity may increase the anisotropic catalytic activity of the crystal faces of the catalyst grain by poisoning a given crystal face, the two grown fibers curl in an opposite direction with a very high curling curvature, and they coalesce together with a high stress. This carbon fiber with a very high curling curvature strongly contributes to form a single-helix carbon nanocoil with a small coil diameter. On the other hand, during the coalescence stage of the two fibers, a very strong inner stress is periodically formed between the boundary of two fibers, and thin carbon films may swell to form the lace-like deposits. Furthermore, these high stress sites may also contribute to nucleation and may activate the growth of secondary fine carbon films and form laces. This may be the reason for the formation of the straight carbon fiber with laces as shown in Fig. 5 and the single-helix carbon nanocoils with laces as shown in Fig. 6.

We may also suggest that when nitrogen gas, which acts as a dilution gas, or say, a sealing gas in case oxygen gets into the reaction tube on both sides, is zero, the concentration of acetylene increases, the deposition speed of the carbon increases, thus the inner stress that periodically forms between the boundary of two fibers is high, resulting in the easier formation of single-helix carbon nanocoils with laces.

4. Conclusions

The carbon nanocoils with various kinds of morphologies were prepared by the catalytic pyrolysis of acetylene using a Ni catalyst supported on molecular sieve containing a trace amount of Fe impurity originating from a kaolin clay raw material. Among these coils, single-helix spring-like carbon coils with laces on the surface were the main product. We found that a trace amount of Fe impurity contained in the molecular sieve was a key factor in the lace growth. We also found that a zero flow rate of the sealing/dilute gas nitrogen is also an important factor. It is considered that the Fe impurity may poison or restrain the formation of three crystal faces resulting in the growth of single helix coils, or activates the anisotropic catalytic activity. It is also considered that a very strong inner stress is periodically formed between the boundary of two fibers, and thin carbon films may swell to form laces.

References

1. I. J. ADADUROV, *J. Phy. Chem. USSR*, **6** (1935) 206.
2. V. IVANOV, A. FONSECA, J. B. NAGY, A. LUCAS, P. LAMBIN and D. BERNAERTS, *Carbon* **33** (1995) 1727.

3. K. HERNADI, A. FONSECA, J. B. NAGY, D. BERNAERTS and A. LUCAS, *Carbon* **34** (1996)1249.
4. P. E. ANDERSON and N. M. RODRIGUEZ, *J. Mater. Res.* **14** (1999) 2912.
5. A. CORMA, *Chem. Rev.* **97** (1997) 2373.
6. D. X. JIANG, N. Y. HE, Y. Y. ZHANG, C. X. XU, C. W. YUAN and Z. H. LU., *Mater. Chem. Phys.* **69** (2001) 246.
7. K. HERNADI, Z. K, A. SISKA, J. KISS, A. OSZK B. NAGY and I. KIRICSI. *ibid.* **77** (2003) 536.
8. S. MOTOJIMA, M. KAWAGUCHI, K. NOZAKI and H. IWANAGA, *Carbon* **29** (1991) 379.
9. X. CHEN and S. MOTOJIMA, *Carbon* **37** (1999)1817.
10. MEI ZHANG, YOSHIKAZU NAKAYAMA and LUJUN PAN, *Jpn. J.Appl. Phys.*, **39** (2000) 1242.
11. LUJUN PAN, TAICHI HAYASHIDA, MEI ZHANG and YOSHIKAZU NAKAYAMA, *ibid.*, **40** (2001) 235.
12. C. KUZUYA, W. IN-HWANG, S. HIRAKO, Y. HISHIKAWA and S. MOTOJIMA, *Chem. Vap. Deposition*, **8** (2002) 57.
13. X. CHEN, S. YANG, K. TAKEUCHI, T. HASHISHIN, H. IWANAGA and S. MOTOJIMA, *Diamond Relat. Mater.* **12** (2003) 1836.
14. S. YANG, X. CHEN and S. MOTOJIMA, *ibid.* **13** (2004) 2152.
15. S. YANG, X. CHEN, S. MOTOJIMA and M. ICHIHARA, *Carbon*, **43**(2005) 827.
16. C. KUZUYA, K. KAWABE and A. UEDA, *Mater. Integration* **17** (2004) 9.
17. X. CHEN, T. SAITO, M. KUSUNOKI and S. MOTOJIMA, *J. Mater. Res.* **14** (1999) 4329.
18. X. CHEN, W. IN-HWANG, S. SHIMADA, M. FUJII, H. IWANAGA and S. MOTOJIMA, *ibid.*, **15** (2000) 808.

*Received 26 December 2004
and accepted 29 June 2005*